NIST ELECTROSTATIC FORCE BALANCE EXPERIMENT

John A. Kramar, David B. Newell, and Jon R. Pratt
National Institute of Standards and Technology, Gaithersburg, MD, USA

We have designed and built a prototype electrostatic force balance for realizing forces in the micronewton range. The active electrodes are concentric cylinders, the outer serving as the reference and the inner suspended and guided by a rectilinear flexure mechanism. The geometry has been designed such that a near-linear capacitance gradient of 1 pF/mm is achieved at a working overlap of 5 mm. We have used this balance in a null-displacement mode to compare an electric realization of force with the force generated by calibrated deadweights of nominal mass 1 mg, 10 mg, and 20 mg. The preliminary measurements reported here agree to within a few parts in 10^4 after including all known correction factors.

Introduction

The trend toward cost-saving and performance enhancement through miniaturization and scale-down in many areas of manufacturing, but particularly in microelectronics, data storage, and micro-electromechanical systems (MEMS), is well known. With this trend comes the increasing need for calibrated force measurements in the micronewton range and below. Many commercial instruments including nanoindenters and atomic force microscopes have force resolutions that extend into the nanonewton regime, and these levels of measurement are becoming increasingly necessary for the control of manufacturing processes. However, no methods for establishing force measurement traceability at these levels are currently available.

Our primary goal is to realize forces in the micronewton to piconewton range. Conceptually, the most straightforward approach would be to use a calibrated mass as a deadweight. However, it is not possible to maintain high levels of precision with this approach as the masses are subdivided. The smallest available calibrated mass is 1 mg (10 μN) having a relative uncertainty at the level of a few parts in 10^4. In principle smaller masses could be calibrated, but they would be difficult to handle, and the achievable relative uncertainty would increase inversely proportionately with the decrease in mass.[1]

Another practical means for realizing forces in this range is through the electrical units defined by the International System of Units (SI). This can be done using electromagnetic forces (*e.g.*, the NIST Watt Balance Experiment [2]) or using electrostatic forces.[3] We have chosen the latter because it is somewhat simpler to execute the required metrology, and the forces generated, although generally less than those feasible electromagnetically, are adequate for the force range of interest. As a validation of our electrostatic force realization, we desire to crosscheck with deadweight forces, at least in our higher force range where the uncertainty achievable mechanically is still competitive. For this reason we have designed our force generator to operate along the vertical axis.

Eventually, the plan is also to design transfer artifacts, *i.e.*, calibrated load cells or force generators, through which we can disseminate this realized force to users in industry or academia.

Experimental Design

We have built a prototype electrostatic force balance that realizes force through the SI electrical units and has the capability of comparing this force with the deadweight force from SI traceable masses.[4] For this first prototype, the design features a spring suspended platen whose deflection can be measured by an interferometer (see Fig. 1). The spring is a beryllium-copper flexure assembly that constrains the platen to rectilinear vertical motion with a spring constant of 13 N/m. The cross-axis stiffness has been measured to be at least 20 times larger. The spring can be deflected either by adding deadweight or by applying an electrostatic force. For comparison between the two, we typically do a null motion experiment: The spring is first held in a deflected position by the application of an electrostatic force. Then a mass is added and the electrostatic force is decreased such that the final platen position is unchanged as measured by the interferometer. The difference in electrostatic forces is then taken to be equal to the deadweight force. The test masses used for this experiment were calibrated against the NIST working standards.

The electrostatic force is generated by applying a voltage across a concentric-cylinder capacitor. The inner cylinder is suspended from the flexure spring. The mechanical work required to change the separation between two electrodes of a capacitor while maintaining constant voltage is

$$dW = F\,dz = \tfrac{1}{2}\,V^2\,dC \qquad (1)$$

where dW is the change in energy, F is the force, dz is the change in separation, V is the electric potential across the capacitor, and dC is the change in capacitance. Thus force can be realized from electrical units by measuring V and the capacitance gradient, dC/dz:

$$F = \tfrac{1}{2}\,(dC/dz)\,V^2. \qquad (2)$$

In our design, the outer diameter of the inner cylinder is 15 mm and the inner diameter of the outer cylinder is 15.8 mm. With this geometry dC/dz is about 1 pF per millimeter of cylinder overlap. We operate at an overlap of 5 mm.

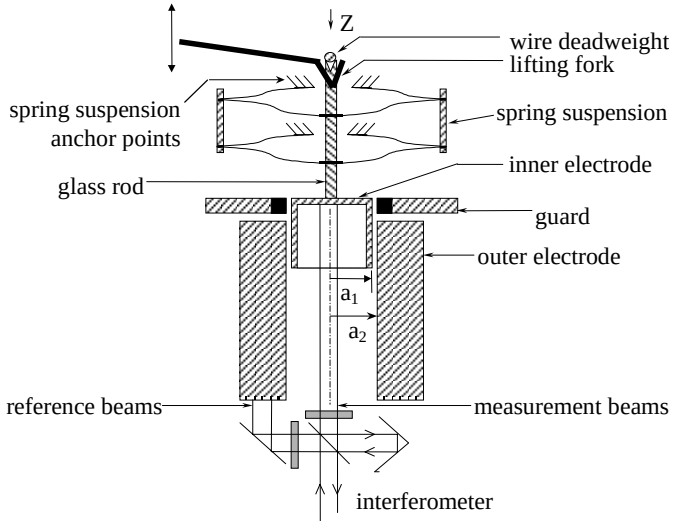

Fig. 1. Schematic block diagram of the NIST electrostatic force balance design.

The operating range of the balance is bracketed by the maximum electrostatic force and the noise floor. The maximum force is limited by the dielectric strength of air to roughly 400 μN. The noise floor is the precision with which null can be held. This is a combination of the noise on the interferometer, the performance of the servo controller, and the vertical flexure stiffness. The interferometer noise and controller performance depend among other factors on the amount of averaging. For our experimental conditions, we measured the force noise floor to be less than 10 nN.

Procedure

The basic weighing procedure is to alternate and bracket weighing sets with measurements of *dC/dz*. This is done under automated software control over periods of time extending to days. Measurements of *dC/dz* are typically done by moving the stage that holds the base of the flexure spring over a range of 400 μm, centered about the weighing null point. The stage is scanned up and down ten times while recording the capacitance and the position at 40 μm intervals. Each up and down cycle is averaged to minimize drift effects (*e.g.,* thermal), and fit by a line to give the slope. These individual gradients are in turn averaged and their standard deviation (type A uncertainty [5]) is calculated to provide an estimate of *dC/dz* at the weighing null point.

For each weighing set, typically 40 mass on/off transitions are performed over a period of 45 min. To minimize any drift effects, the individual weighings are considered to be the difference between the mass on (off) electrostatic force and the mean of the two neighboring mass off (on) electrostatic forces. A rather slow loop time of 125 ms is chosen for the null servo controller to allow time for averaging the interferometer readings and the voltage readings to minimize noise. Furthermore, each mass on (off) voltage is the average of 800 of these servo iterations (100 s). A ring magnet surrounds the inner cylinder to provide eddy current damping of its 12 Hz natural resonance, damping it to a *Q* of 4.2.

Force Comparison and Correction Factors

We compared the deadweight force of the test masses with the electrostatic force. We chose the flexure spring axis along which the inner cylinder motion is constrained as a convenient frame of reference for these force comparisons. The force due to the mass along this axis is given by

$$F_{mf} = - m\, g \cos\theta_{gf}\, B \qquad (3)$$

where m is the mass of the test mass, g is the acceleration of gravity, θ_{gf} is the angle of the flexure axis with respect to gravity, and $B = (1 - \rho_{air}/\rho_{mass})$ is the buoyancy correction, since the electrostatic force balance operates in air. The uncorrected electrostatic force that balances F_{mf} is given by

$$F_{efu} = \tfrac{1}{2} (dC/dz_f) (V_{off}^2 - V_{on}^2) \qquad (4)$$

where dC/dz_f is the capacitance gradient along the flexure-constrained motion axis and V_{on} and V_{off} is the electrostatic potential between the capacitor electrodes with the mass on and off, respectively.

In addition, there are small correction forces due to null-point shift and hysteresis of the flexure spring. These corrections are generally proportional to the applied force. The reference mirror for the interferometer that measures the null position is on the outer

electrode. When the test mass is removed from the platen and the electrostatic force pulling the inner electrode down is increased to hold null position, the outer electrode is also pulled up by the same force. This causes a small shift in the null position equal to $-F_{efu}/k_o$, where k_o is the stiffness of the outer cylinder with respect to this force. This results in less deflection of the inner cylinder and consequently a decrease in the electrostatic force necessary to hold null by an amount equal to $-F_{efu}(k_f/k_o)$, where k_f is the flexure spring compliance. The other correction force we consider is due to spring hysteresis. As the mass is placed on or taken off the platen, there is a transient deflection of the inner-electrode flexure spring due to the slow response of the servo controller. The resulting spring-hysteresis force is an additional force that must be overcome by the electrostatic force. It is dependent on the magnitude and duration of the spring deflection and so is roughly proportional to F_{efu} by an experimentally determined factor h. Taken together, we arrive at a corrected electrically derived force measurement of

$$F_{ef} = F_{efu}\,[1 + (k_f/k_o) - h]. \tag{5}$$

Since the capacitance gradient, dC/dz_f, has a dependence on the centering of the electrodes and other factors including the dielectric constant of air, it is best determined *in situ*, bracketing the sets of mass exchanges. This is done by scanning in z the stage that holds the anchor points of the inner cylinder flexures, as previously discussed. This stage axis, z_s, has previously been aligned to the flexure axis to within a few milliradians. During the scanning for the determination of dC/dz_s, the z motion is measured by the interferometer, which operates along axis z_i. Consequently dC/dz_s is overestimated by $(1/\cos\theta_{si})$ if the interferometer reading is taken as the measure of z_s. We have also done separate experiments to compare dC/dz_f with dC/dz_s. For this, we alternate the usual dC/dz_s measurements with measurements of dC/dz_f, which we obtained by deflecting the flexure axis 160 μm using a 220 mg mass. From this we determine that the capacitance gradients differ by a factor of δ_{sf}, typically about 2.5×10^{-4}. Hence,

$$dC/dz_f = (dC/dz_s)_i\,(1 + \delta_{sf})\cos\theta_{si} \tag{6}$$

where $(dC/dz_s)_I$ is dC/dz_s but with z_s measured along z_i. Combining factors and taking the small angle and small error approximations, we arrive at a mechanically derived force

$$F_{mf} = -\,m\,g\,[1 - (\theta_{gf}^2/2) - \rho_{air}/\rho_{mass}\,] \tag{7}$$

to be compared with an electrically derived force

$$F_{ef} = \tfrac{1}{2}\,(dC/dz_s)_i\,(V_{off}^2 - V_{on}^2)\,[1 + (k_f/k_o) - h + \delta_{sf} - (\theta_{si}^2/2)\,]. \tag{8}$$

Typical numerical values for the correction factors are listed in Table 1.

Results

We have weighed three different test masses multiple times using the electrostatic force balance. The test masses are bent wires with nominal masses 1 mg, 10 mg, and 20 mg, made of Pt, Au and Au, respectively. The uncorrected electrostatic force data, F_{efu}, from a typical data run are shown in Fig. 2. For each set of weighings, the average dC/dz from the two bracketing dC/dz measurements is used. The value, 103 275.8 nN ± 3.3 nN, is the mean and the standard deviation of the individual weighing set averages. So at this force, our fractional type A uncertainty contribution is roughly 30×10^{-6}.

Table 1: Typical correction factors and standard uncertainties, u_c.

Correction Factor	Value ($\times 10^{-6}$)	u_c ($\times 10^{-6}$)
$\theta_{gf}^2/2$	4	4
ρ_{air}/ρ_{mass}	59	5
k_f/k_o	30	5
h	70	70
δ_{sf}	250	250
$\theta_{si}^2/2$	6	4

Table 2: Typical standard uncertainties, u_c, for standard transfers.

Standard Transfer, Q		$u_c = dQ/Q$ ($\times 10^{-6}$)	Uncertainty Type
g		1	B
C		10	
V		6	
z		1	
m	1 mg	380	A and B
	10 mg	38	
	20 mg	19	

The force comparisons with their corresponding uncertainties are listed in Table 3. The data include all the known corrections and uncertainties from Tables 1 and 2. For the mechanical force, the uncertainty is dominated by the uncertainty in the mass, since the uncertainties in the correction factors only contribute a few parts in 10^6. For the electrically derived force, the uncertainties in the correction factors dominate all other sources including the type A contribution from the weighings. All uncertainties are reported as standard uncertainties (coverage factor, $k = 1$). We define the fractional difference as $(F_{ef} - F_{mf})/F_{mf}$. We find that in all cases, the electrically derived force is less than the mechanical force by a few parts in 10^4. For the 10 mg and 20 mg nominal masses, the fractional difference is about -6×10^{-4} whereas the combined uncertainty is a factor of two smaller at 3×10^{-4}. This points to a yet undiscovered systematic error at this level. One possibility we are still exploring, for example, is that dC/dz could be a function of electrostatic potential.

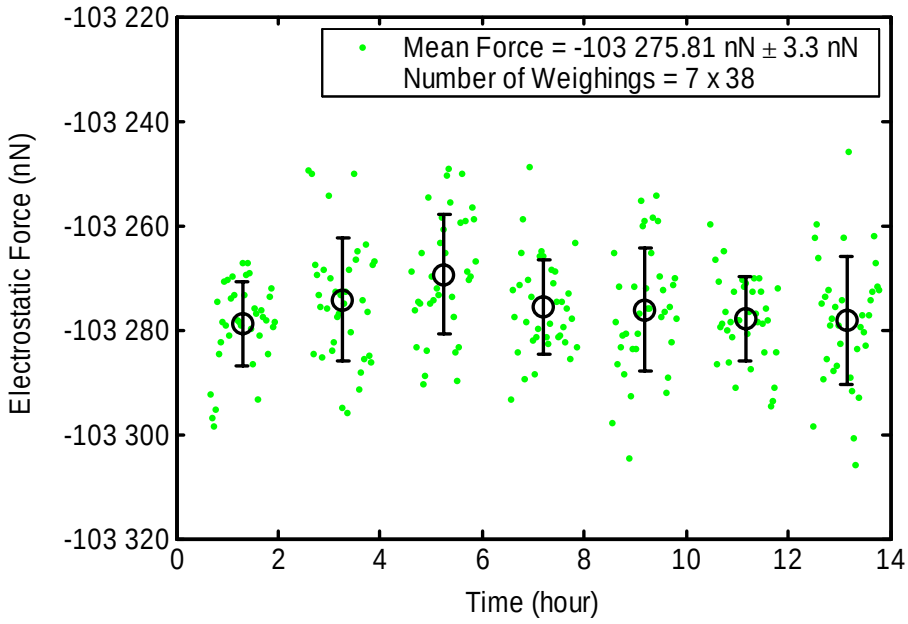

Fig. 2. A typical data run showing the individual uncorrected electrostatic force readings and the mean and uncertainty for each set of weighings.

Table 3: Force comparisons

Nominal mass (mg)	Mechanical Force (μN)	Electrical Force (μN)	Number of Weighing Sets	Fractional Difference (x 10^{-5})	Fractional Uncertainty (x 10^{-5})
1	9.1421(35)	9.1395(37)	13	– 28	56
		9.1385(33)	4	– 39	52
10	103.3057(38)	103.235(30)	12	– 68	30
		103.248(24)	7	– 56	24
20	205.0025(39)	204.898(60)	10	– 51	29

Conclusion

We have successfully built an electrostatic force balance that operates in the micronewton range, and have used it to compare electrically and mechanically derived forces. We have demonstrated an agreement between the two at the level of a few parts in 10^4. Work is in progress to discover the source of the remaining systematic differences. At the same time, we are designing a second prototype balance [6] that will increase our sensitivity, primarily by lowering the vertical spring constant by a factor of 800. It is based on an equal-arm balance design. The smaller spring stiffness will also allow us to measure dC/dz_f more directly by driving the guided inner-cylinder motion using electrostatic forces. This will eliminate the largest correction factor, δ_{sf}, thereby also eliminating the largest source of uncertainty.

References

[1] Jabbour, Z L., and Yaniv, S. L., "The Kilogram and the measurements of mass and force," *Journal of Research of the National Institute of Standards and Technology*, **106**, 2001, pp. 25-46.

[2] Williams, E. R., Steiner, R. L., Newell, D. B., and Olsen, P. T., "Accurate measurement of the Planck constant," *Phys. Rev. Lett.*, **81**, 1998, pp. 2404-2407.

[3] Funck, T. and Sienknecht, V, "Determination of the Volt with the Improved PTB Voltage Balance," *IEEE Trans. on Inst. and Meas.*, **40**(2), 1991, pp. 158-161.

[4] Newell, D. B., Pratt, J. R., Kramar, J. A., Smith, D. T., Feeney, L. A., and Williams, E. R., "SI traceability of force at the nanonewton level," *2001 NCSL International Workshop and Symposium Proceedings, Washington D.C., July 29 – August 2, 2001*.

[5] Taylor, B. N. and Kuyatt, C. E., "Guidelines for evaluating and expressing the uncertainty of NIST measurement results," *NIST Technical Note 1297*, 1994

[6] Pratt, J. R., Newell D. B., and Kramar, J. A., "A flexure balance with adjustable restoring torque for nanonewton force measurement," *(these Proceedings)*, 2002.